Current Research in Pharmacology and Drug Discovery 7 (2024) 100205

Contents lists available at ScienceDirect

Current Research in Pharmacology and Drug Discovery

journal homepage: www.journals.elsevier.com/current-research-in-pharmacology-and-drug-discovery

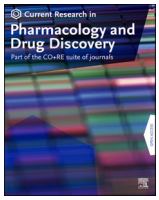

Unveiling the chemotherapeutic potential of two platinum(IV) complexes in skin cancer: *in vitro and in vivo* Insights

Amjad Slika [a], Christina Haydar [a], Joelle Bou Chacra [a], Seba Al Alam [a], Stephanie Mehanna [a], Anthony Lteif [a], Maria George Elias [b], Krishant M. Deo [b], Robin I. Taleb [a], Janice R. Aldrich-Wright [b], Costantine F. Daher [a,c,*]

[a] *School of Arts and Sciences, Department of Natural Sciences, Lebanese American University, Byblos, Mount Lebanon, Lebanon*
[b] *School of Science, Western Sydney University, Locked Bag 1797 Penrith South, 2751, NSW, Australia*
[c] *Alice Ramez Chagoury School of Nursing, Lebanese American University, Byblos, Mount Lebanon, Lebanon*

ARTICLE INFO

Keywords:
Skin cancer
Platinum(IV)
Apoptosis
Selectivity
Chemotherapy

ABSTRACT

The present study investigates the chemotherapeutic potential of two platinum (IV) complexes, P-PENT and P-HEX, against skin cancer *in vitro and in vivo*. Both complexes exhibited potent cytotoxicity against HaCaT-II-4 cells with IC_{50} values of 0.8 ± 0.08 μM and 1.3 ± 0.16 μM respectively, while demonstrating 8-10-fold selectivity compared to mesenchymal stem cells (MSCs). Western blot analysis revealed significant modulation of key apoptotic and survival pathways, including upregulation of Bax/Bcl2 ratio, cleaved caspase 3, and cytochrome *c*, suggesting induction of intrinsic apoptosis. The complexes also inhibited PI3K and MAPK pathways, as evidenced by decreased p-AKT/AKT and p-ERK/ERK ratios. Flow cytometry confirmed significant apoptotic cell death. Both complexes also increased reactive oxygen species production. In a DMBA/TPA-induced skin carcinogenesis mouse model, both complexes significantly suppressed tumor growth at doses considerably lower than the maximum tolerated dose, with no detectable toxicity. A dose escalation study in BALB/c mice showed that P-PENT and P-HEX were approximately 5-fold and 4-fold more tolerated than cisplatin, respectively. In conclusion, the present study provides evidence that P-PENT and P-HEX may have the characteristics of an effective and potentially safe anti-tumor drug that could be used in skin cancer treatment.

1. Introduction

Skin cancer is the most common cancer worldwide, with over 5 million cases diagnosed annually (Apalla et al., 2017). Basal cell carcinoma (BCC) and squamous cell carcinoma (SCC), together termed non-melanoma skin cancers, account for majority of diagnosed cases. As per estimates, approximately 3.3 million cases of BCC and 1 million cases of SCC are diagnosed in the US each year (American Cancer Society, 2022). The major risk factors for development of skin cancers include excessive UV radiation exposure, fair skin, family history, and weakened immune system (Armstrong and Kricker, 2001; Karia et al., 2013). UV radiation, particularly UVB, can directly damage DNA and cause signature mutations in critical genes like p53 tumor suppressor, leading to skin cancer initiation and progression (De Gruijl, 1999). Treatment options for SCC include surgical excision, radiation therapy, topical/systemic chemotherapy, photodynamic therapy and immunotherapy (Aboul-Fettouh et al., 2021). Mohs micrographic surgery is considered optimal, allowing complete microscopic margin evaluation during tumor removal. Radiation is used for cases where surgery is difficult or combined with chemotherapy/immunotherapy for advanced tumors. Topical chemotherapy creams containing 5-fluorouracil are commonly prescribed for superficial lesions (Stătescu et al., 2023).

Cisplatin was the first platinum anticancer drug, discovered accidently in 1965 (Rosenberg et al., 1969). Platinum (II) complexes like cisplatin typically have a square planar geometry, with two amine ligands and two labile ligands arranged in a cis orientation (Wang and Lippard, 2005). Such complexes exert cytotoxic effects by entering cells and binding DNA, causing intra-strand and inter-strand crosslinks that trigger apoptosis (Jamieson and Lippard, 1999). However, cisplatin treatment is associated with severe toxicities including nephrotoxicity, neurotoxicity, ototoxicity, and myelosuppression (Dasari and

* Corresponding author. Department of Natural Sciences, School of Arts and Sciences, Lebanese American University, Lebanon.
E-mail address: cdaher@lau.edu.lb (C.F. Daher).

https://doi.org/10.1016/j.crphar.2024.100205
Received 27 May 2024; Received in revised form 30 August 2024; Accepted 21 October 2024
Available online 26 October 2024

Tchounwou, 2014). Many cancers also develop resistance to cisplatin, limiting its efficacy (Galluzzi et al., 2011). These issues led to the development of second (carboplatin, oxaliplatin) and third generation (satraplatin, picoplatin) platinum drugs.

More recently, platinum (IV) complexes have gained attention as promising anti-cancer agents due to their flexible structural framework relative to their platinum (II) analogues (Johnstone et al., 2016). Platinum (IV) complexes are octahedral rather than square planar, with the formula ML2X2R2 - two leaving groups (X), two inert ligands (L), and two axial ligands (R) (Johnstone et al., 2016). The additional axial ligands on platinum (IV) centers enable chemists to fine tune a variety of ligand frameworks to enhance structure-activity-relationship (SAR) through enhanced lipophilic properties as well as an increased affinity to multiple cellular targets (Kenny et al., 2017). Early platinum (IV) drugs like ormaplatin and satraplatin showed efficacy against cisplatin-resistant cancers, prompting clinical trials (Rose et al., 1982; Rahman et al., 1988). However, rapid reduction to reactive platinum (II) caused neurotoxicity, preventing Phase II progression (Schilder et al., 1994; O'Rourke et al., 1994). Current strategies use physiologically active ligands, rather than halogens, as leaving groups (Johnstone et al., 2016). These ligands target non-DNA sites, thus avoiding resistance to DNA-targeting platinum (II) analogues that are released upon reduction (Johnstone et al., 2016). Such dual functional ligands not only enhance the cytotoxic activity of the parent platinum (IV) prodrug, but they also reduce the potential for cellular resistance (Kenny et al., 2017).

Our lab has focused on developing novel platinum (II) and platinum (IV) complexes with altered axial ligands that have greater potency and tumor selectivity compared to existing drugs. In one study, our lab reported chloro-substituted polyaromatic platinum (II) complex Pt12Cl2 and its platinum IV analogue, which showed 14-fold higher activity than cisplatin in lung cancer cells (Baz et al., 2024). Another study conducted by Khoury et al. (2022) showed that the platinum IV complex (47OMESS (IV)) showed 17–22-fold greater selectivity toward the cancerous cells compared to the non-cancerous MCs. Also, previous research conducted by Deo et al. (2019) reported the synthesis and characterization of novel platinum (IV) complexes with axial ligands of increasing lipophilicity. The complexes exhibited nanomolar cytotoxicity against several cancer cell lines, with some showing over 850-fold greater activity than cisplatin, particularly against colon cancer. Therefore, the aim of this study is to expand the scope of this research and evaluate the cellular uptake, distribution and chemotherapeutic potential and safety of two of these novel platinum (IV) complexes, P-PENT and P-HEX, on skin cancer *in vitro* and *in vivo* (Fig. 1).

2. Methods

2.1. Materials and reagents

Cell culture reagents including DMEM, fetal bovine serum, PBS, trypsin, and antibiotics were purchased from Sigma Aldrich without further purification. Chemicals including Triton X-100, SDS, Tween 20, BSA, DMBA, TPA, Tris, and NaOH were purchased from Fisher Scientific, and Bio-Rad. Kits for assessing apoptosis (Guava Nexin) and ROS (DCFDA/H2DCFDA) were purchased from Sigma-Aldrich and Abcam. Solutions and buffers were prepared including RIPA lysis buffer, acrylamide gels from Bio-Rad, Tris buffers at pH 6.8 and 8.8, running buffers, transfer buffers, TBS, TBST, blocking buffer, and electrophoresis solutions. Antibodies purchased from Abcam targeted proteins involved in apoptosis and cell signaling.

2.2. Cell lines

The HaCaT-II-4 cell line were purchased from Cytion that were originally isolated from the spontaneously transformed keratinocytes of histologically normal skin obtained from a 62-year-old adult donor. Mesenchymal Stem Cells (MSCs) were extracted from rats' bone marrow. All cells were cultured in DMEM supplemented with 10 % Fetal Bovine Serum (FBS) and 1 % penicillin-streptomycin in a humidified cell incubator with 5 % CO_2 at 37 °C.

Cytotoxicity of P-PENT, P-HEX, and Cisplatin on HaCaT-II-4 and MS cells.

HaCaT-II-4 cells (passage 15) and MSCs were cultured and plated in 96 well plates at a confluency of 10,000 cells/100 μL in each well then were treated with either P-HEX, P-PENT, or cisplatin (positive control) using a 3-fold serial dilution DMEM at a starting concentration of 150 μM (0.023, 0.069, 0.206, 0.617, 1.85, 5.56, 16.67, 50 and 150 μM) for 72 h. Media were then removed and 100 μL of fresh DMEM followed by 10 μL of WST-1 reagent (4-[3-(4-iodophenyl)-2-(4- nitro-phenyl)-2H-5-tetrazolio]-1,3-benzene sulfonate) (water-soluble tetrazolium salt) was applied for 4 h at 37 °C. Absorbance was measured at 450 nm using the VarioskanTM LUX Multimode microplate reader to determine cell viability. The experiment was conducted in three independent trials each triplicated.

2.3. Mesenchymal stem cell extraction

Mesenchymal stem cells were extracted from 12-week-old rats provided at the animal facility at the Lebanese American University. The animals were kept under optimal temperature and humidity conditions with proper access to food and water. The study protocol, which was a modified version of a previously described method (Smajilagić et al., 2013) followed the Guide for the Care and Use of Laboratory Animals and were approved by Animal Care and Use Committee (LAU.ACUC. SON.CD1.23/January/2023). In brief, rats were euthanized using CO_2 asphyxiation, and both hind legs were removed under aseptic conditions. The femoral and tibial bones were isolated, cleaned with ethanol, and rinsed with 1% PBS. Using a needle containing DMEM supplemented with 10% FBS and 1.5% penicillin-streptomycin, the bone marrows were flushed out. The collected cells were then cultured at 37 °C with 5% CO_2 then were identified using an inverted light microscope (Nikon Eclipse TE300) as having spindle like morphology before being used for experiments.

2.4. Ultraviolet–visible (UV) spectroscopy

UV spectroscopy experiments were conducted, using an Agilent

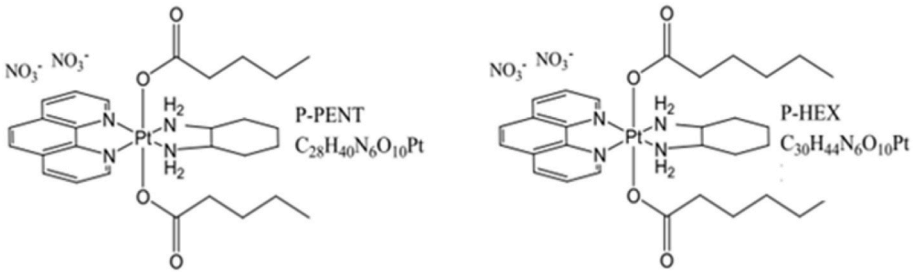

Fig. 1. Chemical structures of the novel platinum IV complexes P-PENT and P-HEX.

Technologies Cary 3500 UV–Vis Multicell Peltier spectrophotometer, to determine the stability of the complexes. Each of the complexes was dissolved in either ultra-pure water, PBS, or DMEM at a concentration of 100 μM. Spectra were recorded (room temperature) at 0, 1, and 24 h over a range of 250–400 nm using a 1 cm quartz cuvette. All experiments were performed in triplicate. Spectra were baseline corrected, and average peak areas were recorded.

2.5. Quantification of cellular uptake

HaCaT-II-4 cells were plated in 6 well plates at a concentration of 2 $\times$ 10^5 cells/well. Cells were left to adhere overnight at 37 °C and 5% CO_2, after which a concentration of 3 μM of either P-PENT, P-HEX, or Cisplatin was applied. After 1, 3, 6, 12, 24, and 30 h, media were removed and each well was washed thrice with cold phosphate buffer saline (PBS) and left to dry. Cells were then digested for 75 min with 400 μL of 60 % HNO_3. The digests were transferred to 15 ml conical that were previously filled with 7 ml of 0.05 μM internal standard indium solution, followed by milliQ water addition to reach a final volume of 14 ml with a final concentration of 2 % HNO_3. Cellular uptake was quantified by ICP-MS based on internal and external standards, indium and platinum respectively. The experiment was conducted in three independent trials each triplicated. The data was averaged from all trials and optimized following a calibration curve and expressed in nM/10^6 cells.

2.6. Cellular fractionation

HacaT-II-4 cells were cultured in 6-well plates and allowed to adhere overnight at 37 °C and 5% CO_2, then treated with 3 μM concentration of either P-PENT, P-HEX, or Cisplatin for 24 h. Media were then removed and the wells were washed thrice with cold PBS. The process of isolating and fractionating the cells was performed according to the instructions provided by the cell fractionation kit (Cell signaling technology, USA, #9038). Initially, cells were detached using trypsin and collected through centrifugation at 350*g* for 5 min at 4 °C. The resulting pellet was suspended in cold PBS and centrifuged at 500 g for 5 min at 4 °C. After removing the supernatant, the cytoplasm isolation buffer (100 μL) was added to the pellet, and the mixture was vortexed for 5 s, kept on ice for 5 min then centrifuged at 500 g for 5 min. The resulting supernatant represented the cytoplasmic fraction (CF). The pellet was then suspended in the membrane isolation buffer (100 μL), vortexed for 15 s, kept on ice for 5 min, and centrifuged at 8000 g for 5 min. The membrane and organelle fraction (MO) is in the supernatant. Finally, the pellet was re-suspended in the cytoskeleton/nucleus isolation buffer (50 μL) to form the nuclear and cytoskeletal fraction (NC). Subsequently, samples from all three fractions were completely evaporated at 100 °C and then incubated with concentrated HNO_3 (200 μL) for 1.5 h. After that, ultrapure water was added to reach a final volume of 7 mL, containing 0.025 μM indium. The resulting solution was filtered, and the platinum complexes were quantified using ICP-MS.

2.7. ROS detection

The DCFDA/H2DCFDA-cellular ROS Assay Kit (Abcam, Cambridge, USA) was used to determine the presence of reactive oxygen species (ROS) in treated cells. HaCaT-II-4 cells were plated in 96-wells plates at a concentration of 25,000 cells/ml, left to adhere overnight, then treated with 3 μM concentration of P-PENT or P-HEX for 72 h or with 150 μM of TBHP (tert-butyl hydroperoxide; positive control) for 4 h. Media were removed and cells stained with DCFDA (25 μM) for 45 min at 37 °C and 5% CO_2. Wells were then washed with 1x Kit buffer, and 100 μL of phenol red free media was added before scanning the plate to measure the fluorescence at an excitation/emission spectrum of 485/535 nm using the VarioskanTM LUX Multimode microplate reader (ThermoFisher).

2.8. Cell death analysis through flow cytometry

Annexin V-Phycoeryhtrin (Annexin V-PE) and 7-AAD (7-amino-actinomycin D) staining (Guava Nexin Reagent Kit, Luminex, Austin, Texas, U.S.A) were used to analyze and detect the mode of death of HaCaT-II-4 cells 48 and 72 h post treatment with the platinum complexes. Cells were cultured and plated in 6 well plates (10^5 cells/ml), left to adhere overnight and then treated with either P-PENT, P-HEX, or cisplatin (3 μM) for 48 h or 72 h at 37 °C and 5% CO_2. Cells were harvested, dissolved in 100 μL Guava Nexin Reagent buffer and then pipetted into 96 well plates and incubated in dark for 10 min. Reading was done using the Guava easyCyte 8HT Benchtop Flow Cytometer and Annexin V/7-AAD data was measured on FL1-H versus FL2-H scatter plot.

2.9. Western blot

HaCaT-II-4 cells (2×10^5 cells/well) were plated on 6 well plates and then treated with either P-HEX, P-PENT, or cisplatin (3 μM) for 72 h. Proteins were then extracted, heated at 95 °C (5 min), and loaded to 10% SDSPAGE for 60 min at 80 V and for 60 min at 120 V. The gels were transferred to a PVDF membrane (Pall Corporation, Ann Arbor, USA), blocked with blocking buffer (1 $\times$ TBS, 0.1% Tween 20, 5% skim milk) for 1 h after which the membranes were probed with primary antibodies at 4 °C overnight. The following primary antibodies were used: Bcl-2 (1:2000; rabbit; Invitrogen PA5-27094), Bax (1:2000; rabbit; Invitrogen MA5-32031), Cytochrome C (1:2000; rabbit; Invitrogen PA5-86022), Pro-Caspase-3 (1:2000, rabbit, PA5-96077), Cleaved-Caspase-3 (1:500; rabbit; Invitrogen PA5-1146,871), Erk (1:1000; rabbit; Invitrogen MA5-15134), p-ERK (1:000; rabbit; Invitrogen MA5-36265), Cleaved-Caspase 9 (1:1000; rabbit; Invitrogen PA5-105271), p-AKT (1:1000; rabbit; Invitrogen PA5-104869), AKT (1:1000; rabbit, Invitrogen PA5-77855), Actin (Internal Reference; 1:1000; rabbit; Cell Signaling Technology #4970). Membranes were then washed thrice (5 min) with TBST, treated with secondary antibodies (90 min), and washed thrice (10 min) with TBST afterward. The protein bands immunoreactive to the antibodies were detected using the chemiluminescence ECL kit from Bio-Rad (U.S.A.). Blot images were captured and obtained with the BioRad ChemiDoc Imaging system. Band intensities were normalized to the β-actin loading control and quantified using Image Lab 5.2.1 software.

2.10. Experimental animals

Adult female BALB/c mice (21–24 g; 8–12 weeks old) were obtained from the animal facility at the Lebanese American University. The animals were kept under optimum temperature (22 $\pm$ 2 °C) and humidity (50 $\pm$ 5%), with an alternating light and dark cycles of 12-hr. Animals were provided with a standard laboratory diet and free access to water. All experimental procedures were approved by the ACUC at the Lebanese American University (LAU.ACUC.SON.CD1.23/January/2023) and followed the guidelines for the care and usage of laboratory animals set by the National Research Council Committee in the USA.

2.11. Determination of the most tolerated dose

The maximum tolerated dosage (MTD) of P-PENT and P-HEX was determined using female mice aged 8–10 weeks. Mice (n = 3) received intraperitoneal injections (IP) of the complexes in escalating dosages starting with a dose of 5 mg/kg body weight and were monitored for any adverse behavioral or physiological modifications. If no such changes were observed, animals were given a higher dose of the complexes. This process was repeated, increasing the dosage each time, until undesirable changes in behavior were noted. The MTD was considered as the highest dose administered that did not cause any behavioral or physical effects.

2.12. Toxicity study

Adult female BALB/c mice (n = 6 per group) received weekly IP injections (25 mg/kg) of P-PENT, P-HEX, or ultrapure water (negative control). Behavioral modifications, weight alterations, and fatality incidence were observed over 6 weeks. At the end of the experiment, animals were euthanized using CO_2 inhalation, blood samples were collected with cardiac puncture and organs harvested and weighed. Serum samples were analyzed for alanine aminotransferase (ALT), aspartate aminotransferase (AST), alkaline phosphatase (ALP), lactate dehydrogenase (LDH), total Bilirubin, creatinine and blood urea nitrogen.

2.13. Skin cancer induction and treatment

Skin cancer was produced in BALB/c female mice (10-week-old) using an altered DMBA/TPA chemical carcinogenesis procedure (Wiśniewski et al., 2009). Papilloma formation was initiated through a single topical application of 200 nmol of DMBA in 0.2 ml acetone on the shaved dorsal skin. Between week 2 and 7, tumor formation was promoted using 40 nmol TPA in 0.2 ml acetone applied (2 times/week) to the same dorsal region. At week 8, another DMBA treatment was administered followed by TPA application from week 9 until the end of the experiment. Tumor diameters were measured weekly with a Vernier caliper. Once tumors reached the desired volumes (>1–2 mm in diameter), mice were subdivided into groups of four animals each and treated once a week for 6-week (IP) with either P-PENT, P-HEX, or Cisplatin (positive control). Treatment doses were 5, 15, or 25 mg/kg body weight for P-PENT and P-HEX groups and 2.5 mg/kg of body weight for the cisplatin group, while the control group got weekly IP injection of ultrapure water. Tumor diameters were measured weekly during treatment and photos taken at the beginning (weeks 0) and end (week 6) of the treatment period. Tumor volumes were calculated using V = (W2 x L)/2 (V = volume, W = width, L = length) (Faustino-Rocha et al., 2013). After six weeks of treatment, mice were weighed, sacrificed using CO_2 inhalation and organ weights were recorded.

2.14. Statistical analysis

Data were statistically analyzed using one-way analysis of variance (ANOVA). The results for each parameter in the experiments are expressed as Mean ± SEM. For multiple comparisons, Bonferroni post hoc test was used to identify significant main effect differences. All analyses were conducted with SPSS 18, and differences among groups were deemed statistically significant if $p < 0.05$

3. Results

3.1. Cytotoxicity on hacat-ii-4 and MS cells

The cytotoxic effects of P-PENT, P-HEX, and cisplatin were assessed against HaCaT-II-4 and MS cells 72 h post-treatment (Fig. 2). P-PENT and P-HEX showed significantly higher cytotoxicity against HaCaT-II-4 cells (IC_{50} values of 0.8 ± 0.08 μM and 1.3 ± 0.16 μM respectively) compared to MSC extracted from rat bone marrow (IC_{50} values of 8.7 ± 0.55 μM and 7.2 ± 0.27 μM respectively). Cisplatin, however, exhibited more cytotoxicity against MSC (IC_{50} 3.7 ± 0.13 μM) when compared to HaCaT-II-4 cells (IC50 of 6.7 ± 0.76 μM). The IC_{50} of P-PENT and P-HEX against HaCaT-II-4 cells were respectively 8.4 and 5.1 folds lower than that of Cisplatin.

3.2. Cellular uptake

Cellular uptake was quantified using ICP-MS based on internal (Indium) and external (Platinum) standards. Results (Fig. 3A) showed a time dependent uptake of all complexes reaching a maximum at 24 h (P-PENT: 1267 nmol/10^6 cells; P-HEX: 1777 nmol/10^6 cells; cisplatin: 380 nmol/10^6 cells). Calculation of the intracellular to extracellular ratio for all three complexes revealed a very high intracellular accumulation (Fig. 3B). Compared to cisplatin, P-PENT and P-HEX showed a significantly higher uptake and maximum intracellular to extracellular ratio (3.5 folds, P-PENT; 4.5 folds, P-HEX).

3.3. Intracellular distribution

Cellular fractionation assay was used to detect the intracellular distribution of P-PENT, P-HEX, and Cisplatin in the cytoplasmic fraction (CF), membrane and organelle (MO), and nuclear and cytoskeletal (NC) fractions of HaCaT-II-4 cells (Fig. 4). All complexes showed the highest accumulation in the MO fraction (47% for all complexes), followed by the CF fraction (38%, 35%, and 30%), then the NC fraction (15%, 20%, 25%) for cisplatin, P-PENT and P-HEX respectively.

3.4. Quantification of reactive oxygen species (ROS) production

ROS production in HaCaT-II-4 cells was quantified 72 h post-treatment with 3 μM concentration of P-PENT or P-HEX, with TBHP as positive control. Results (Fig. 5) showed that both complexes significantly increased ROS production by ~2-folds as compared to the control group.

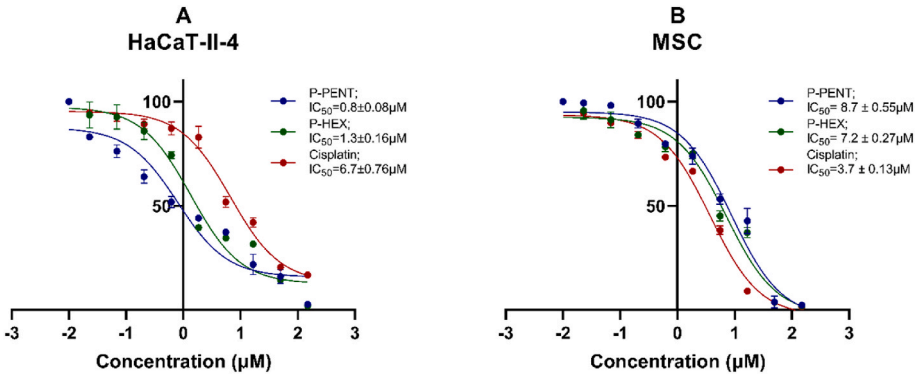

Fig. 2. Cytotoxicity of P-PENT, P-HEX and Cisplatin in HaCaT-II-4 cells (A), and MSCs (B). Percent cell survival was assessed 72 h post-treatment with P-PENT, P-HEX, or cisplatin using a 3-fold serial dilution starting at 150 μM. Data are presented as mean ± SEM of 3 independent experiments, where samples are run in triplicates.

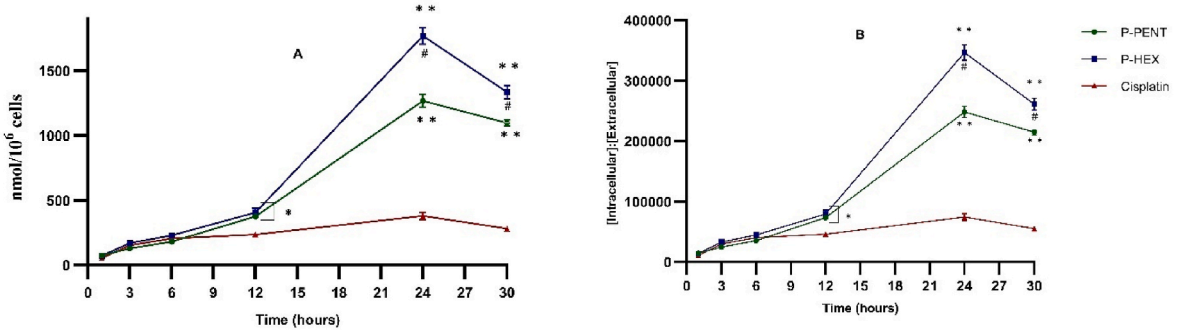

Fig. 3. Uptake of P-HEX, P-PENT, or Cisplatin in HaCaT-II-4 cells using ICP-MS. (A) Represents the cellular uptake of the complexes in nmol per 10^6 cells. (B) Represents the ratio of intracellular to extracellular concentrations for each complex. Error bars denote standard errors of the mean (SEM). Data points are derived from three independent experiments performed in triplicates (n = 3). *($p < 0.01$) and **($p < 0.0001$) denote significant difference between P-PENT and Cisplatin or P-HEX and Cisplatin. #($p < 0.01$) denotes significant difference between P-PENT and P-HEX.

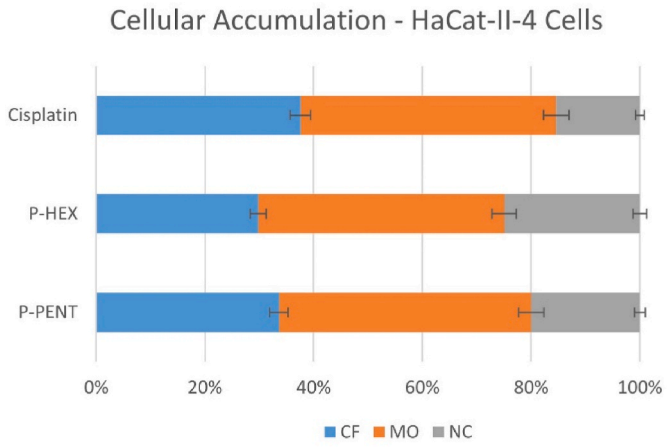

Fig. 4. Cellular accumulation of P-PENT, P-HEX, or cisplatin in HaCaT-II-4 cells. The bar graphs represent the percentage of platinum complexes in different cellular fractions 24 h post-treatment. Bars denote mean ± SEM from three independent experiments run in triplicates.

3.5. Cell death analysis

To evaluate the type of cell death in HaCaT-II-4 cells post-treatment (48 h and 72 h) with P-PENT, or P-HEX (cisplatin as a positive control), cells were stained with Annexin-V/7AAD and detected using flow cytometry (Fig. 6). Both complexes and cisplatin caused a significant ($p < 0.0001$) increase in both early and late apoptosis when compared to the negative control. The percentage of late apoptotic cells observed for P-PENT and P-HEX at 72 h was higher than that at 48 h.

3.6. Western blots analysis

Western blot was conducted to detect key apoptotic proteins in HaCaT-II-4 cells treated with either P-PENT, P-HEX, or cisplatin for 48 h (Fig. 7). Protein bands were all quantified and normalized over actin. Results showed a significant upregulation in the pro-apoptotic proteins BAX, BAX/BCl_2 ratio, cleaved caspase 9, cleaved caspase 3 and cytochrome *c*. The levels of p-AKT, p-AKT/AKT ratio, p-ERK, and p-ERK/ERK ratio were significantly downregulated.

3.7. Most tolerated dose

The most tolerated dose was considered as the maximum dose before any physical or behavioral change is observed in the treated animals. A dose escalation study carried out in mice showed (Table 1) that the MTD

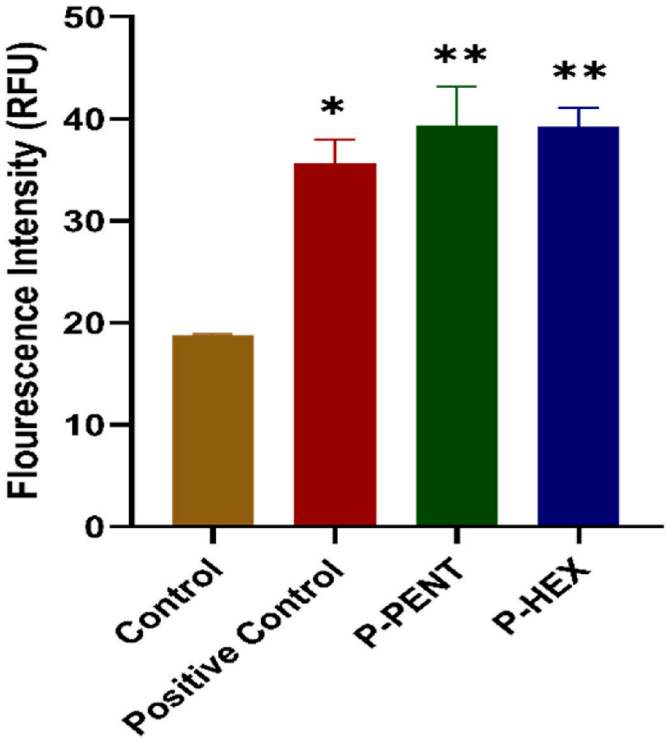

Fig. 5. Effects of P-PENT or P-HEX on ROS production. Cells were treated for 72 h with 3 μM concentration of P-PENT or P-HEX. The positive control was generated using TBHP for 4 h. Bars represent mean ± SEM from 3 independent experiments. *($p < 0.01$) and **($p < 0.001$) implies significant difference between treatment and control groups.

values for both P-PENT and P-HEX are 75 mg P-PENT/Kg (18.75 mg Pt/Kg) and 60 mg P-HEX/Kg (14.40 mg Pt/Kg) of body weight respectively.

3.8. Toxicity study

To evaluate the effect of the complexes on kidney and liver functions, a toxicity study was conducted. Mice were injected (IP) on a weekly basis, for 6 weeks, with either P-PENT or P-HEX (25 mg/kg). At the end of the treatment period, serum analysis of key liver enzymes (Alanine aminotransferase, Aspartate aminotransferase, Alkaline phosphatase, LDH, and total Bilirubin) and key kidney markers (creatinine and blood urea nitrogen) showed no significant difference between either of the treated groups relative to the negative control group (Fig. 8).

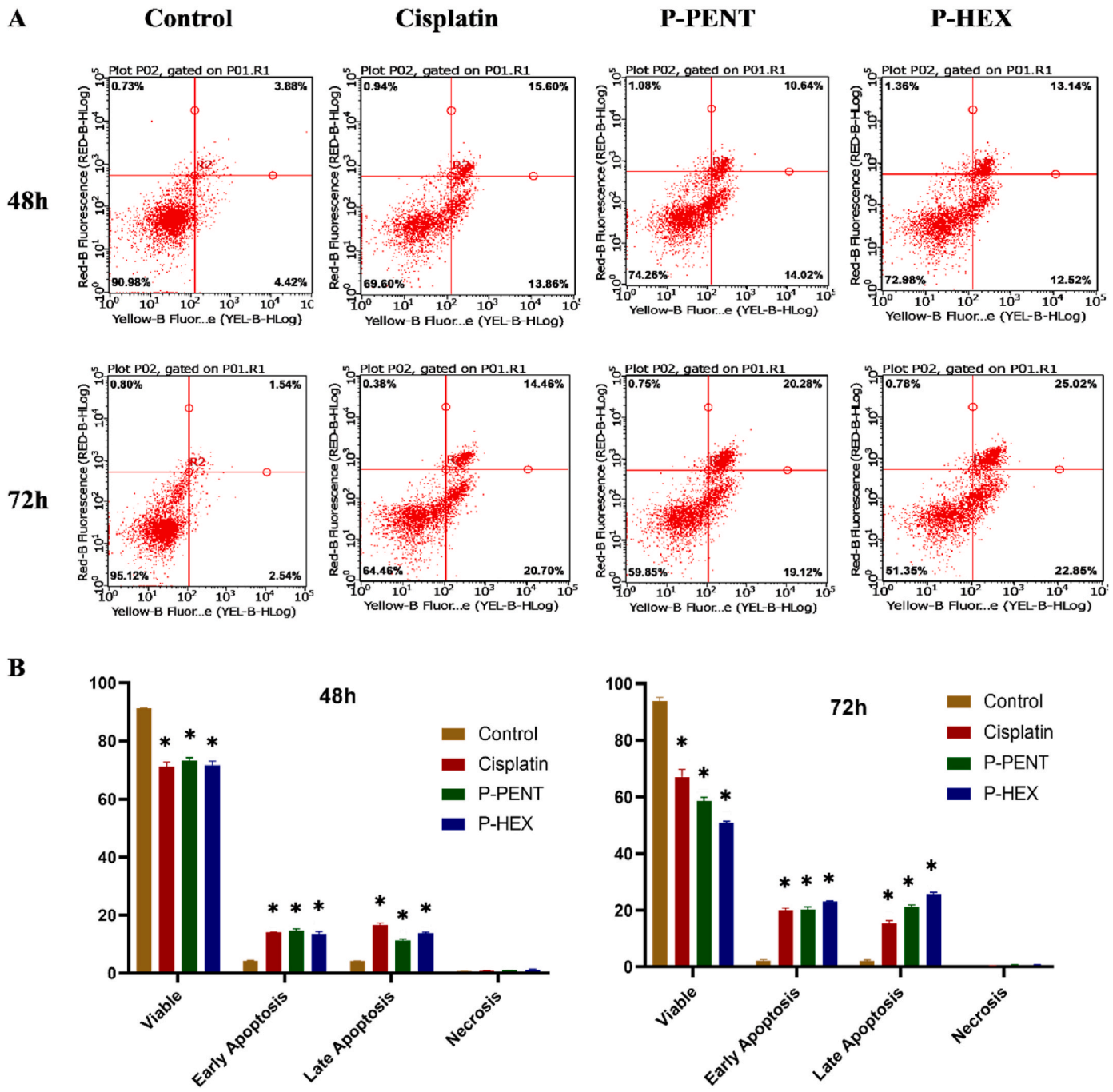

Fig. 6. HaCaT-II-4 cell death analysis 48 h and 72 h post-treatment with P-PENT, P-HEX, or cisplatin. Cells were stained with Annexin-V/7AAD staining and the percentage distribution of cell death (early apoptosis, late apoptosis, necrosis) was determined using flow cytometry. Data are presented using representative dot plots (A) and bar graphs (B) where bars denote mean ± SEM from 3 independent experiments run in triplicates. *($p < 0.0001$) implies significant difference between treated and control groups.

3.9. Chemotherapeutic potential on skin cancer

To evaluate the chemotherapeutic effect of P-PENT, P-HEX, and cisplatin, a DMBA/TPA induced skin carcinogenesis mouse model was used (Fig. 9). Compared to control, all treated groups exhibited a significant decrease in tumor volume starting week 4 with the exception of the P-PENT group (25 mg/kg of body weight) which started at week 3 post treatment ($p < 0.001$). Although a dose dependent trend (albeit slightly) was observed between 5 and 15 mg/kg doses of P-PENT, yet that dose dependency was less pronounced beyond this range. P-HEX, however, exhibited no dose dependency across the three-dose range. Representative images showing animal samples from each group at day 0 and week 6 post treatment are shown in Fig. 10. None of the treatment groups showed a significant change in body or organ (lungs, kidneys, heart, liver, brain, and spleen) weights post dissection (Fig. S1).

4. Discussion

In the present study, we aim to assess the anticancer efficacy and safety of two platinum (IV) complexes in skin cancer using *in vitro and in vivo* models. With a common framework comprising of diaminocyclohexane and phenathroline ligands, the two complexes

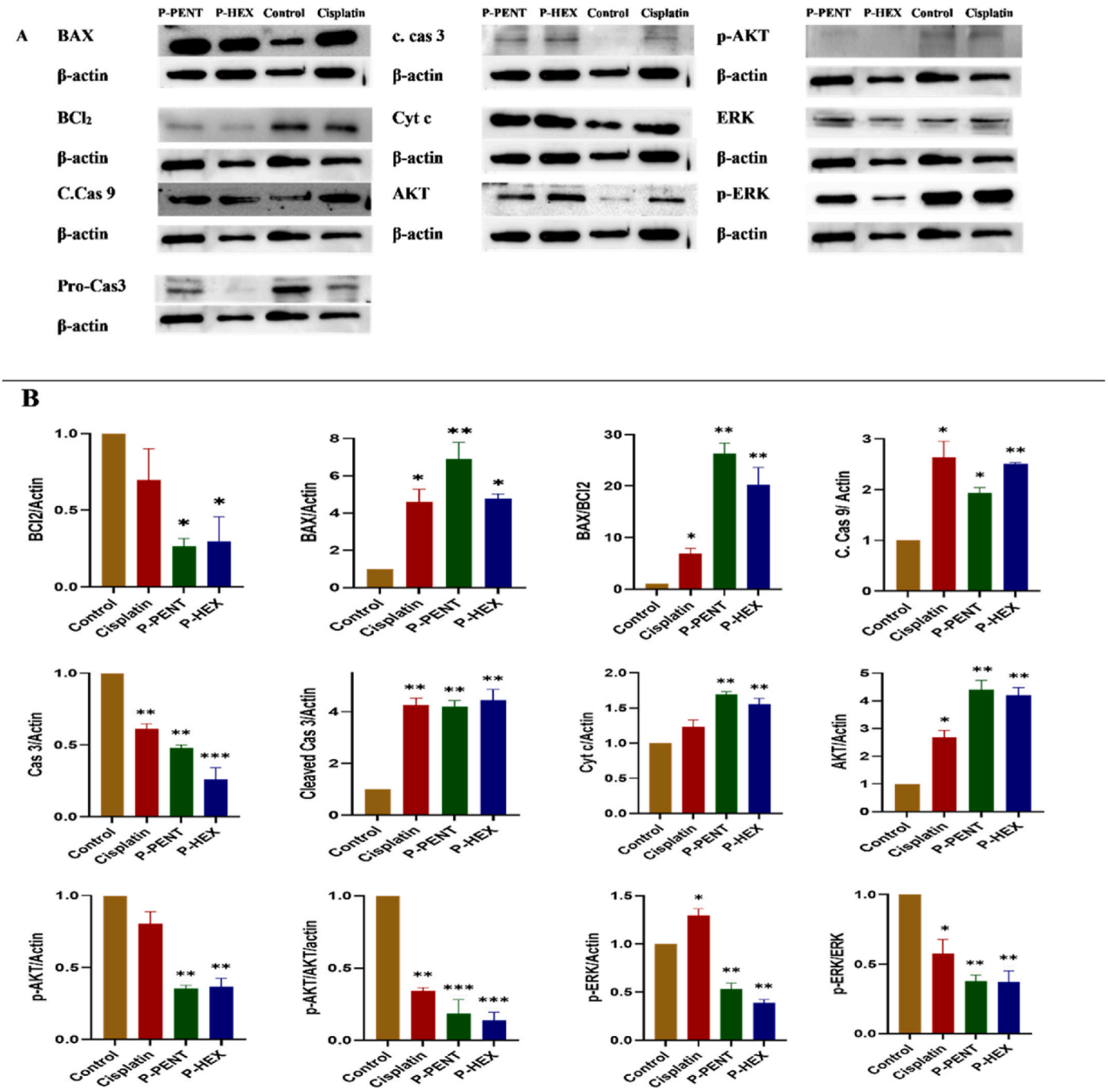

Fig. 7. Western blot results showing the expression of key apoptotic proteins in HaCaT-II-4 cells 48 h post-treatment with P-PENT, P-HEX, or Cisplatin. A) Representative Western blot images for BAX, Bcl2, cleaved caspase 9, caspase 3, cleaved caspase 3, cytochrome *c*, AKT, p-AKT, ERK, and p-ERK. B) densitometric graphs, illustrating the effect of P-PENT, P-HEX, or Cisplatin treatment on the apoptotic markers in HaCaT-II-4 cells. *($p < 0.05$), ** ($p < 0.01$), ***($p < 0.001$) denoted significant difference compared to the control. Bars represent mean ± SEM, with $n = 3$ from three independent experiments.

however differ on the axial positions where either a pentanoate (P-PENT) or hexanoate (P-HEX) ligand is attached. Cell viability assay showed significant cytotoxicity of P-PENT and P-HEX against HaCaT-II-4 cells with IC_{50} values in the low micromolar range. These findings are in line with previous results on these complexes against other cancer cell lines (Deo et al., 2019). Compared to HaCaT-II-4 cells, P-PENT and P-HEX exhibited 8 to 10-folds less cytotoxicity against MSCs extracted from rat bone marrow. These results support the potential selectivity of the two complexes towards cancer. Cisplatin, however, showed ~2-folds higher cytotoxicity against rat bone marrow MSCs when compared to HaCaT-II-4 cells. This finding corroborates with the reported side effects observed with cisplatin use as a chemotherapeutic drug (Johnstone et al., 2016).

In order to confirm the studied platinum complexes' selectivity against cancer cells, a dose escalation (to determine the most tolerated dose – MTD) and 6-week toxicity studies were conducted using BALB/c mice. The MTD values for P-PENT and P-HEX were 18.75 mg Pt/Kg and 14.40 mg Pt/Kg respectively. The lower MTD observed with P-HEX could be attributed to its higher intracellular accumulation as compared to P-PENT. Aston et al. (2017), however, reported an MTD value for cisplatin of 3.9 mg Pt/Kg in BALB/c mice, which is 4-to-5-folds less than that observed with the tested complexes. These results further support

Table 1
Dose escalation study in BALB/c mice.

P-PENT			P-HEX		
Dose		Behavioral Change	Dose		Behavioral Change
mg Pt/Kg	mg/Kg		mg Pt/Kg	mg/Kg	
1.25	5	No	1.20	5	No
2.50	10	No	2.40	10	No
5.00	20	No	4.80	20	No
7.50	30	No	7.20	30	No
11.25	45	No	10.80	45	No
15.00	60	No	**14.40**	**60**	**No**
18.75	**75**	**No**	18.00	75	Yes
22.50	90	Yes	15.60	65	Yes
20.00	80	Yes	19.20	80	–

the observed *in vitro* selectivity of the four complexes. Additionally, the 6-week toxicity study conducted on BALB/c mice using P-PENT and P-HEX revealed that both complexes have no significant effect on liver (ALT, AST, ALP, and total Bilirubin) and kidney functions (creatinine and blood urea nitrogen) compared to control. The high MTD and the low toxicity of the tested complexes is noteworthy as it suggests selectivity and wider therapeutic window of the complexes compared to cisplatin. The MTD of common platinum-based complexes like Oxaliplatin and Carboplatin were 20 mg/kg (9.82 mg Pt/Kg) and 60 mg/kg (31.53 mg Pt/Kg) of body weight in mice (O'Dwyer et al., 1985; Korst et al., 1997).

The cellular uptake, assessed using ICP-MS, showed time-dependency with maximum accumulation of P-PENT and P-HEX attained at 24 h. It was not possible to increase the incubation time to more than 30 h due to the significant increase in cell death seen beyond 30 h of treatment. Both tested complexes exhibited significantly higher uptake when compared to cisplatin in HaCaT-II-4 cells. Such an observation may be attributed to the incorporation of the lipophilic ligands in the complexes, which results in faster and more intracellular accumulation alongside their improved cytotoxicity (Wang & Guo, 2013; Wilson and Lippard, 2013). Calculation of the intracellular to extracellular ratio of the complexes supports an active mode of transport due to their very high intracellular accumulation. These finding are in line with previous studies carried out at our lab on lung cancer cells (A549) treated with **Pt(II)5ClSS** and **Pt(IV)5ClSS** (Baz et al., 2024) as well as on other platinum-based complexes (Hall et al., 2008; Howell et al., 2010; Burger et al., 2011).

The stability of both complexes was evaluated in ultra-pure water, PBS, and DMEM using UV spectroscopy over a wavelength range of 250–400 nm at 0, 1, and 24 h. Spectral analysis revealed no significant reduction in peak areas at either 1 or 24 h, indicating robust stability in the studied solvents (Table S1). Given that maximum cellular uptake was observed at 24 h post-treatment, it can be inferred that complex reduction does not occur in the extracellular media. Instead, the reduction process is likely predominantly intracellular, where reducing conditions prevail, lending further support to the proposed mechanism of action for these platinum (IV) complexes which are designed to remain stable in circulation and undergo activation upon entering the reducing intracellular environment (Johnstone et al., 2016; Chen et al., 2024).

The intracellular distribution of the complexes in the cytoplasmic (CF), membrane and organelle (MO), and nuclear and cytoskeletal (NC) fractions was assessed using ICPMS. Both P-PENT and P-HEX were distributed among the three cellular fractions with both being largely

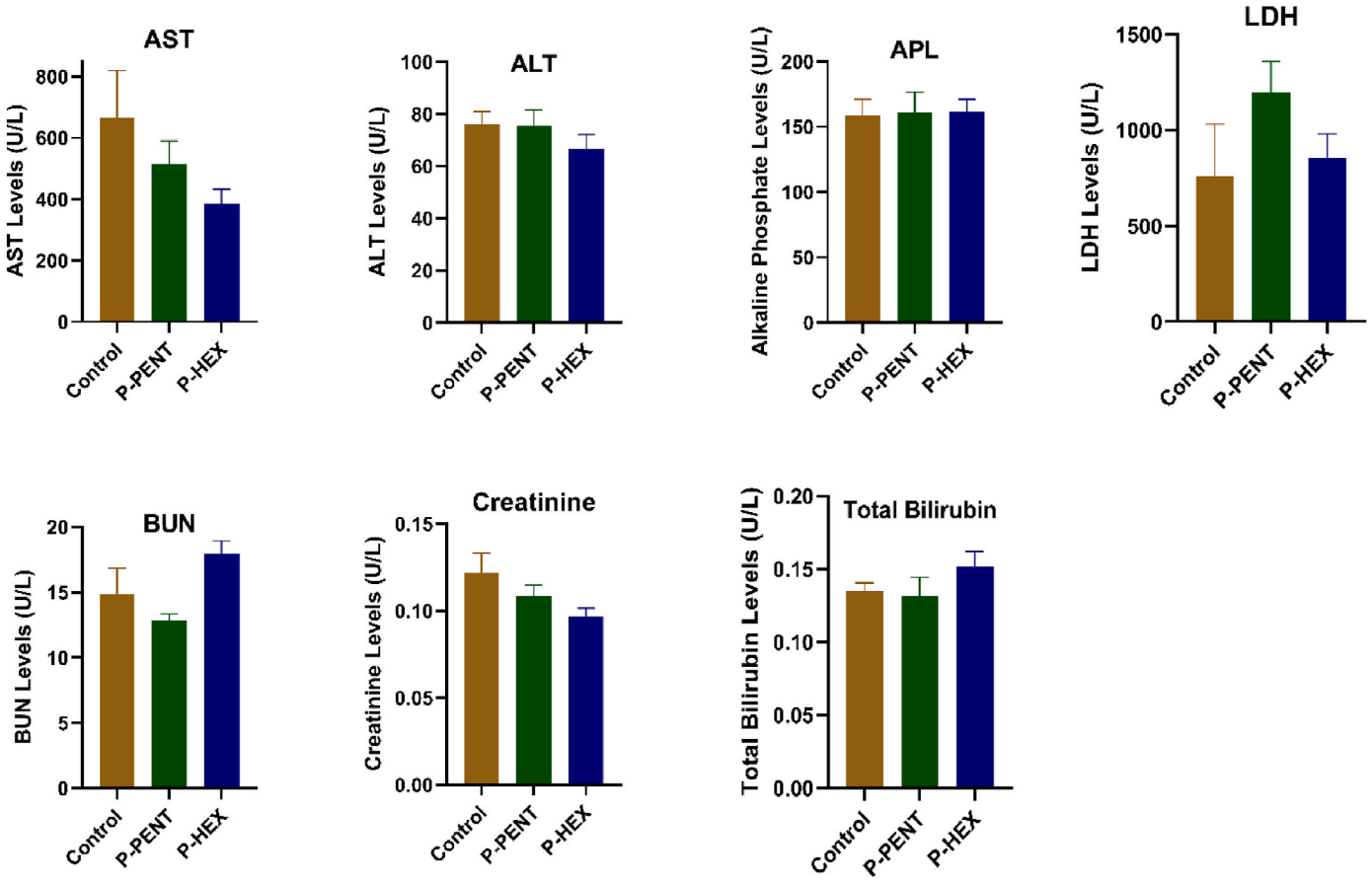

Fig. 8. Serum levels of Alanine aminotransferase, aspartate aminotransferase, alkaline phosphatase, total bilirubin, creatinine, and blood urea nitrogen of mice treated for 6 weeks with P-PENT or P-HEX. Bars represent mean ± SEM (n = 6).

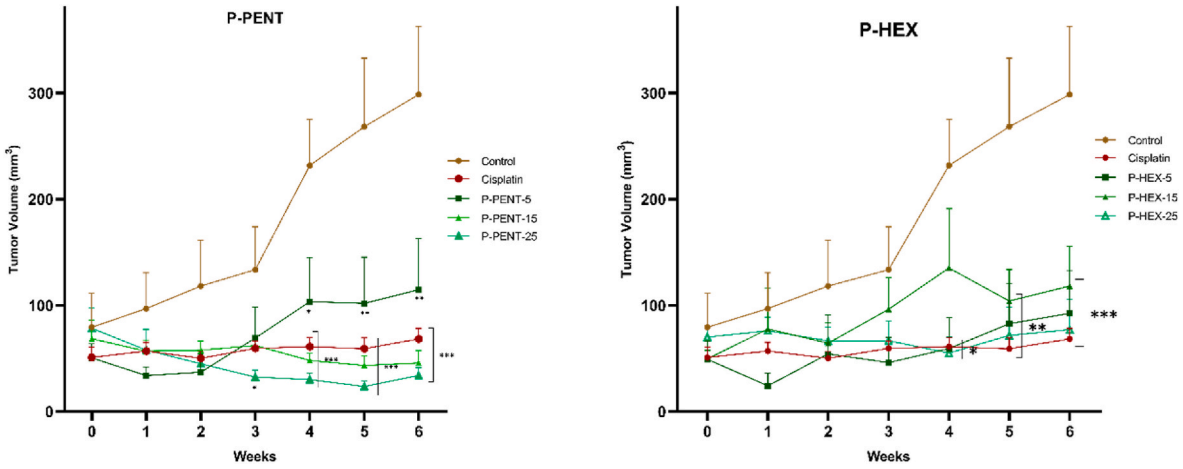

Fig. 9. Effects of P-PENT, P-HEX, and cisplatin treatment on tumor volume. Mice were treated intraperitoneally for 6 weeks with P-PENT/P-HEX (5, 15, or 25 mg/kg body weight), or cisplatin (2.5 mg/kg body weight). Data points represent mean ± SEM (n = 5). *($p < 0.01$), ** ($p < 0.001$), ***($p < 0.0001$) denote a significant difference between treatment and control groups.

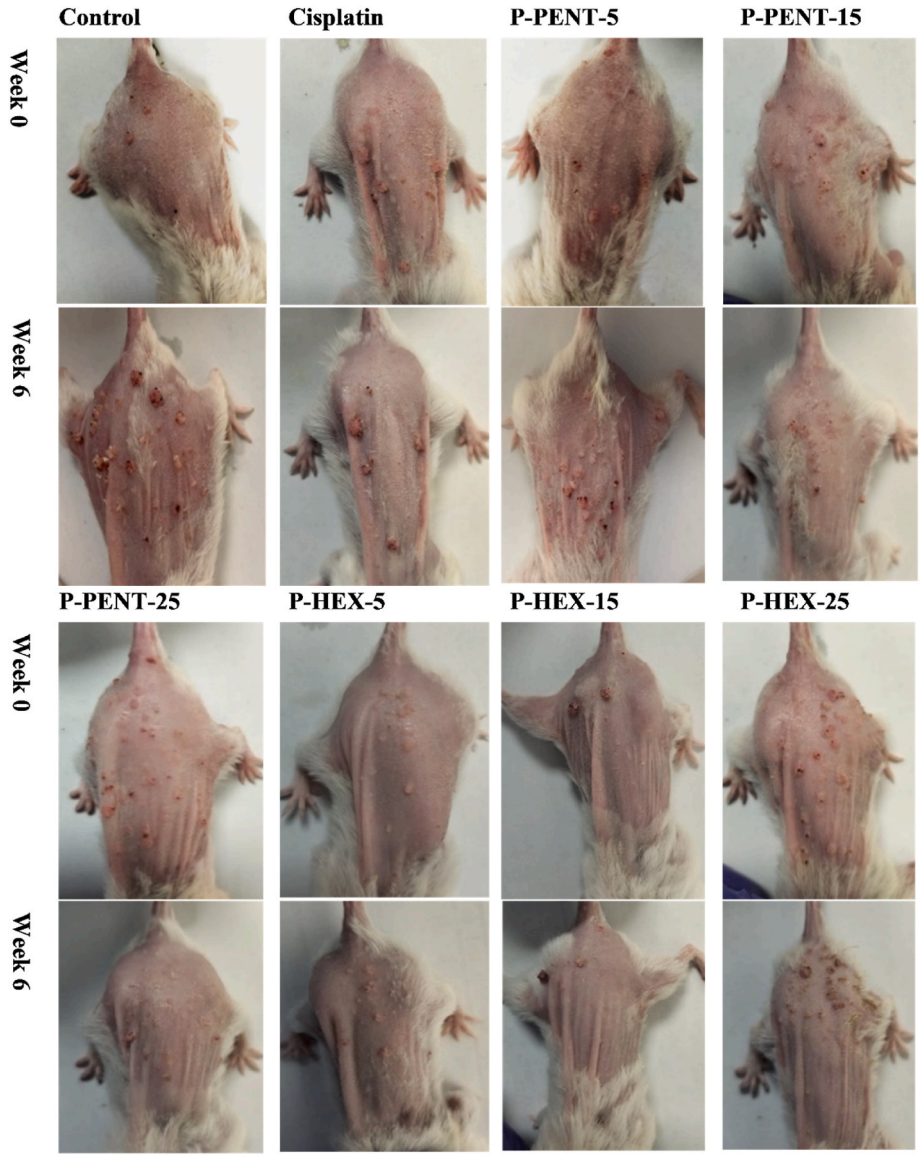

Fig. 10. Tumor images for mice treated with P-PENT, P-HEX, or Cisplatin. Mice were treated for 6 weeks, intraperitoneally, with 5, 15, or 25 mg/kg of P-PENT and P-HEX, or 2.5 mg/kg of cisplatin. Images were taken at week 0 and week 6 and compared to the control group. The table shows images of 4 mice from each group.

accumulated in the MO fractions in HaCaT-II-4 cells, similar to cisplatin. These results differ from our previously reported platinum (II) and platinum (IV) complexes where accumulation was largely observed in the NC fraction (Baz et al., 2024; Khoury et al., 2022). It is worth mentioning that a large amount of each of P-PENT and P-HEX is significantly (20%: P-PENT; 25%: P-HEX) localized in the NC fraction. The distribution of the platinum complexes among the various cellular fractions suggests a multi-mechanistic role that could be exploited in combination therapy to help overcome the issue of cancer cell resistance.

Previous reports have demonstrated that platinum complexes have the ability to trigger apoptosis in various cancer cells (Cregan et al., 2012; Dasari and Tchounwou, 2014; Khoury et al., 2022). This mechanism is often dysregulated in cancer cells, which allows them to evade cell death and continue proliferating (Pistritto et al., 2016; Ghobrial et al., 2005). HaCaT-II-4 cells were treated with P-PENT, P-HEX, or cisplatin for 48 or 72 h and then subjected to flow cytometry analysis. Data revealed a significant increase in apoptosis, particularly early and late apoptosis. A clear transition from early to late apoptosis was also noted for P-PENT and P-HEX with prolonged incubation time. No evidence of significant necrosis was observed. Using Western blot, 48 h post treatment, the expression of Bcl-2, BAX, caspase-3, cytochrome *c*, AKT, p-AKT, and p-ERK was investigated in HaCaT-II-4 cells. Interestingly, cells treated with P-PENT and P-HEX had significantly higher levels of the pro-apoptotic protein BAX and significantly lower levels of the anti-apoptotic protein Bcl-2. The BAX/Bcl-2 ratio, which is a critical predictor of apoptotic activation (Shamas-Din et al., 2013), increased significantly in P-PENT, P-HEX and cisplatin treated cells. These results are consistent with prior research indicating the role of Bcl-2 family proteins in platinum-induced apoptosis (Wilkins et al., 2012; Baz et al., 2024). The elevated BAX/Bcl-2 ratio is known to increase the mitochondrial membrane permeability leading to cytochrome *c* release and shifting the balance toward pro-apoptotic signaling (Wang, 2001). The release of cytochrome *c* from the mitochondria into the cytosol is a critical event in the intrinsic apoptotic pathway (Wang, 2001) as it results in the creation of the apoptosome complex, which triggers the activation of caspase-9 and, later, caspase-3 (Li et al., 1997). In the present study, the significant upregulation of cytochrome *c* expression in P-PENT and P-HEX-treated cells suggests that these complexes may trigger apoptosis via the mitochondrial route (intrinsic pathway). These results are also consistent with previous published data showing the elevated levels of cytochrome *c* in platinum-based therapy (Baz et al., 2024). The cleavage of caspase-3, a major executioner caspase in the apoptotic pathway (Shalini et al., 2014), is an essential indicator of apoptosis. The considerable downregulation of pro-caspase-3 and elevation of cleaved caspase-3 in treated cells with P-PENT and P-HEX suggests an activation of the caspase cascade required for apoptosis (Salvesen, 2010). The AKT and ERK signaling pathways play key roles in cell survival, growth, and death (Meng et al., 2017; Fan et al., 2007). In the present study, the significantly lower p-AKT/AKT ratio indicates that these complexes may block the AKT survival pathway and contribute to the apoptosis-inducing actions of P-PENT and P-HEX. Similarly, the significant decrease in p-ERK/ERK levels observed with P-PENT and P-HEX treatment, suggests that these complexes may also block the ERK survival pathway. These results align with previous data showing the impact of platinum complexes on modulating the MAPK pathway (Al-Khayal et al., 2020). P-PENT and P-HEX, therefore, partly exert their anticancer activity through inhibition of the MAPK and PI3K signaling pathways.

The formation of reactive oxygen species (ROS) is considered a significant metabolic pathway responsible for the toxic effects exerted by platinum drugs (Choi et al., 2015; Trachootham et al., 2009). ROS are reactive molecules that cause damage to several cellular components such as DNA and proteins, disturbing the function and fragility of the cell, ultimately leading to cell death (Birben et al., 2012). In this study, treatment of both HaCaT-II-4 cells with P-PENT and P-HEX for 72 h led to a significant increase in ROS production compared to the control. These results confirm that both complexes cause oxidative stress which may in part contribute to their cytotoxic activity. TBHP was used a positive control instead of cisplatin.

In order to evaluate the *in vivo* chemotherapeutic effect of the complexes, a DMBA/TPA-induced skin cancer model in mice was used. This model mimics the multistage processes of carcinogenesis which allow researchers to evaluate the chemopreventive and chemotherapeutic potential of investigated complexes (Abel et al., 2009; Abba et al., 2016; Plante, 2021; Daaboul et al., 2018; Shebaby et al., 2020). In the present investigation, skin tumors were chemically induced, and after reaching at least 1–2 mm in diameter, a six-week treatment period was conducted using the platinum complexes. Data revealed that treatment with either P-PENT, P-HEX, or cisplatin, significantly decreased the average skin tumor volume compared to the control starting 3–4 weeks post treatment. The three complexes were able to suppress tumor growth over the 6 weeks of treatment, with P-PENT slightly outperforming the anticancer activity of both P-HEX and cisplatin. Although a dose-dependent trend of anticancer activity was observed with P-PENT treatment (but not P-HEX), there were no significant differences among the three different doses used. The lack of significant difference between the 5 mg/kg dose of P-PENT and the remaining doses, especially toward the end of the treatment period, could be attributed to the large variation in the efficacy of this dose. Extending the treatment period to more than 6 weeks could have resulted in a significant difference between the 5 mg/kg and the 15 or 25 mg/kg doses. The relatively similar and consistent anticancer efficacy noted with the 15 and 25 mg/kg doses of P-PENT indicates that the optimum dose lies within that range. The MTD for P-PENT (75 mg/kg) and P-HEX (60 mg/kg) are 3 and 2.4 folds higher than the highest doses used in the present *in vivo* study respectively. This probably justifies why no adverse effects was recorded during the 6 weeks of treatment with both platinum complexes. We could not increase the treatment dose of cisplatin to more than 2.5 mg/kg as its MTD value is 6 mg/kg of body weight (Aston et al., 2017). Also, preliminary data in our lab revealed that a 5 mg/kg cisplatin dose causes significant mortality in BALB/c mice after few weeks of treatment. Therefore, the ability of the two complexes to significantly suppress tumor growth highlights their potential anticancer activity and broad-spectrum efficacy if considered in future clinical trials. Furthermore, the different chemical structures and properties of these complexes may provide unique mechanisms of action and resistance pathways in comparison with cisplatin (Johnstone et al., 2016). This is of great of importance because a major problem in cancer chemotherapy is the formation of drug resistance, which may eventually decrease the effectiveness of anticancer drugs (Housman et al., 2014). Hence, the platinum complexes under study may have the potential to bypass the cisplatin resistance mechanism by using a different set of targets or cellular pathways.

In conclusion, P-PENT and P-HEX displayed an active mode of transport and exhibited a potent anti-neoplastic activity and selectivity toward HaCaT-II-4 cancer cells. This anticancer property of the complexes is multi-mechanistic as it is attributed to the significant production of ROS, induction of an intrinsic apoptotic pathway and inhibition of the MAPK and PI3K pathways. The selectivity and antineoplastic activity of the complexes were also evident *in vivo* since both complexes suppressed tumor growth in chemically induced skin cancer model while causing no observed toxicities. The present study, therefore, provides evidence that P-PENT and P-HEX may have the characteristics of a potent and potentially safe anti-tumor drug that could be of benefit in skin cancer treatment.

Funding sources

The authors acknowledge the financial support from the President Intramural Research Fund at the Lebanese American University (PIRF I0006).

CRediT authorship contribution statement

Amjad Slika: Software, Validation, Formal analysis, and, Investigation, Data curation, Writing – original draft, Preparation, All authors have read and approved to the published version of the manuscript. **Christina Haydar:** Methodology. **Joelle Bou Chacra:** Methodology. **Seba Al Alam:** Methodology. **Stephanie Mehanna:** Methodology, Validation, Formal analysis, and, Investigation, Supervision. **Anthony Lteif:** Methodology, Validation, Formal analysis, and, Investigation. **Maria George Elias:** Methodology, Validation, Formal analysis, and, Investigation. **Krishant M. Deo:** Methodology. **Robin I. Taleb:** Conceptualization, Resources, Data curation, Writing – review & editing, Supervision, Project administration. **Janice R. Aldrich-Wright:** Conceptualization, Data curation, Writing – review & editing, Supervision, Project administration. **Costantine F. Daher:** Conceptualization, Methodology, Resources, Data curation, Writing – review & editing, Supervision, Project administration.

Declaration of competing interest

The authors declare that they have no known competing financial interests or personal relationships that could have appeared to influence the work reported in this paper.

Acknowledgments

We would also like to thank Mr Elias Abi Ramia for assisting with animal care and handling in the animal facility at the Lebanese American University.

Appendix A. Supplementary data

Supplementary data to this article can be found online at https://doi.org/10.1016/j.crphar.2024.100205.

Data availability

Data will be made available on request.

References

Abba, M.C., Zhong, Y., Lee, J., Kil, H., Lu, Y., Takata, Y., et al., 2016. DMBA induced mouse mammary tumors display high incidence of activating Pik3caH1047 and loss of function Pten mutations. Oncotarget 7, 64289–64299.

Abel, E.L., Angel, J.M., Kiguchi, K., DiGiovanni, J., 2009. Multi-stage chemical carcinogenesis in mouse skin: fundamentals and applications. Nat. Protoc. 4, 1350–1362.

Aboul-Fettouh, N., Morse, D.C., Patel, J., Migden, M.R., 2021. Immunotherapy and systemic treatment of cutaneous squamous cell carcinoma. Dermatol. Pract. Concept. 11, e2021169S.

Al-Khayal, K., Vaali-Mohammed, M.-A., Elwatidy, M., Traiki, T.B., Al-Obeed, O., Azam, M., et al., 2020. A novel coordination complex of platinum (PT) induces cell death in colorectal cancer by altering redox balance and modulating MAPK pathway. BMC Cancer 20. https://doi.org/10.1186/s12885-020-07165-w.

American Cancer Society, 2022. Key Statistics for Basal and Squamous Cell Skin Cancers. Retrieved from Cancer. org website: https://www.cancer.org/cancer/basal-and-squamous-cell-skin-cancer/about/key-statistics.html.

Apalla, Z., Lallas, A., Sotiriou, E., Lazaridou, E., Ioannides, D., 2017. Epidemiological trends in skin cancer. Dermatol. Pract. Concept. 7. https://doi.org/10.5826/dpc.0702a01.

Armstrong, B.K., Kricker, A., 2001. The epidemiology of UV induced skin cancer. J. Photochem. Photobiol. B Biol. 63, 8–18.

Aston, W.J., Hope, D.E., Nowak, A.K., Robinson, B.W., Lake, R.A., Lesterhuis, W.J., 2017. A systematic investigation of the maximum tolerated dose of cytotoxic chemotherapy with and without supportive care in mice. BMC Cancer 17. https://doi.org/10.1186/s12885-017-3677-7.

Baz, J., Khoury, A., Elias, M.G., Mansour, N., Mehanna, S., Hammoud, O., et al., 2024. Enhanced potency of a chloro-substituted polyaromatic platinum(II) complex and its platinum(IV) prodrug against lung cancer. Chem. Biol. Interact. 388, 110834.

Birben, E., Sahiner, U.M., Sackesen, C., Erzurum, S.C., Kalayci, Ö., 2012. Oxidative stress and antioxidant defense. World Alle. Org. J. 5, 9–19.

Burger, H., Loos, W.J., Eechoute, K., Verweij, J., Mathijssen, R.H.J., Wiemer, E.A.C., 2011. Drug transporters of platinum-based anticancer agents and their clinical significance. Drug Resist. Updates 14, 22–34.

Chen, S., Zhou, Q., Ng, K.-Y., Xu, Z., Xu, W., Zhu, G., 2024. Advances in technical strategies for monitoring the reduction of Platinum(IV) complexes. Inorg. Chem. Front. 11, 3085–3118.

Choi, Y.-M., Kim, H.-K., Shim, W., Anwar, M.A., Kwon, J.-W., Kwon, H.-K., et al., 2015. Mechanism of Cisplatin-Induced cytotoxicity is correlated to impaired metabolism due to mitochondrial ROS generation. PLoS One 10, e0135083.

Cregan, I.L., Dharmarajan, A.M., Fox, S.A., 2012. Mechanisms of cisplatin-induced cell death in malignant mesothelioma cells: role of inhibitor of apoptosis proteins (IAPs) and caspases. Int. J. Oncol. 42, 444–452.

Daaboul, H.E., Dagher, C., Taleb, R.I., Bodman-Smith, K., Shebaby, W.N., El-Sibai, M., et al., 2018. The chemotherapeutic effect of β-2-himachalen-6-ol in chemically induced skin tumorigenesis. Biomed. Pharmacother. 103, 443–452.

Dasari, S., Tchounwou, P.B., 2014. Cisplatin in cancer therapy: molecular mechanisms of action. Eur. J. Pharmacol. 740, 364–378.

De Gruijl, F.R., 1999. Skin cancer and solar UV radiation. Eur. J. Cancer 35, 2003–2009.

Deo, K.M., Sakoff, J., Gilbert, J., Zhang, Y., Wright, J.R.A., 2019. Synthesis, characterisation and influence of lipophilicity on cellular accumulation and cytotoxicity of unconventional platinum(iv) prodrugs as potent anticancer agents. Dalton Trans. 48, 17228–17240.

Fan, Y., Chen, H., Qiao, B., Luo, L., Ma, H., Li, H., et al., 2007. Opposing effects of ERK and p38 MAP kinases on HeLa cell apoptosis induced by dipyrithione. Mol. Cells/Mol. Cell. 23, 30–38.

Faustino-Rocha, A.I., Oliveira, P.A., Pinho-Oliveira, J., Teixeira-Guedes, C., Soares-Maia, R., Da Costa, R.M.G., et al., 2013. Estimation of rat mammary tumor volume using caliper and ultrasonography measurements. Lab. Anim. 42, 217–224.

Galluzzi, L., Senovilla, L., Vitale, I., Michels, J., Martins, I., Kepp, O., Castedo, M., 2011. Molecular mechanisms of cisplatin resistance. Oncogene 31, 1869–1883.

Ghobrial, I.M., Witzig, T.E., Adjei, A.A., 2005. Targ. apoptosis path. canc. ther. Ca 55, 178–194.

Hall, M.D., Okabe, M., Shen, D.-W., Liang, X.-J., Gottesman, M.M., 2008. The role of cellular accumulation in determining sensitivity to Platinum-Based chemotherapy. Annu. Rev. Pharmacol. Toxicol. 48, 495–535.

Housman, G., Byler, S., Heerboth, S., Lapinska, K., Longacre, M., Snyder, N., Sarkar, S., 2014. Drug resistance in cancer: an overview. Cancers 6, 1769–1792.

Howell, S.B., Safaei, R., Larson, C.A., Sailor, M.J., 2010. Copper transporters and the cellular pharmacology of the Platinum-Containing cancer drugs. Mol. Pharmacol. 77, 887–894.

Jamieson, E.R., Lippard, S.J., 1999. Structure, recognition, and processing of Cisplatin−DNA adducts. Chem. Rev. 99, 2467–2498.

Johnstone, T.C., Suntharalingam, K., Lippard, S.J., 2016. The next generation of platinum drugs: targeted PT(II) agents, nanoparticle delivery, and PT(IV) prodrugs. Chem. Rev. 116, 3436–3486.

Karia, P.S., Han, J., Schmults, C.D., 2013. Cutaneous squamous cell carcinoma: estimated incidence of disease, nodal metastasis, and deaths from disease in the United States, 2012. J. Am. Acad. Dermatol. 68, 957–966.

Kenny, R.G., Chuah, S.W., Crawford, A., Marmion, C.J., 2017. Platinum(IV) Prodrugs – a step closer to Ehrlich's vision? Eur. J. Inorg. Chem. 2017, 1596–1612.

Khoury, A., Elias, E., Mehanna, S., Shebaby, W.N., Deo, K., Mansour, N., et al., 2022. Novel platinum(II) and platinum(IV) antitumor agents that exhibit potent cytotoxicity and selectivity. J. Med. Chem. 65, 16481–16493.

Korst, A., Boven, E., Van Der Sterre, M., Fichtinger-Schepman, A., Van Der Vijgh, W., 1997. Influence of single and multiple doses of amifostine on the efficacy and the pharmacokinetics of carboplatin in mice. Br. J. Cancer 75, 1439–1446.

Li, P., Nijhawan, D., Budihardjo, I., Srinivasula, S.M., Ahmad, M., Alnemri, E.S., Wang, X., 1997. Cytochrome c and dATP-dependent formation of apaf-1/caspase-9 complex initiates an apoptotic protease cascade. Cell 91, 479–489.

Meng, Y., Wang, W., Kang, J., Wang, X., Sun, L., 2017. Role of the PI3K/AKT signalling pathway in apoptotic cell death in the cerebral cortex of streptozotocin-induced diabetic rats. Exp. Ther. Med. 13, 2417–2422.

O'Dwyer, P.J., Leyland-Jones, B., Alonso, M.T., Marsoni, S., Wittes, R.E., 1985. Etoposide (VP-16–213). New England J. Medicine/~the œNew England J. Medicine 312, 692–700.

O'Rourke, T.J., Weiss, G.R., New, P., Burris, H.A., Rodriguez, G.I., Eckhardt, J., et al., 1994. Phase I clinical trial of ormaplatin (tetraplatin, NSC 363812). Anti Cancer Drugs 5, 520–526.

Pistritto, G., Trisciuoglio, D., Ceci, C., Garufi, A., D'Orazi, G., 2016. Apoptosis as anticancer mechanism: function and dysfunction of its modulators and targeted therapeutic strategies. Aging 8, 603–619.

Plante, I., 2021. Dimethylbenz(a)anthracene-induced mammary tumorigenesis in mice. In: Methods in Cell Biology, pp. 21–44.

Rahman, A., Roh, J.K., Wolpert-DeFilippes, M.K., Goldin, A., Venditti, J.M., Woolley, P. V., 1988. Therapeutic and pharmacological studies of tetrachloro(d,l-trans)1,2-diaminocyclohexane platinum (IV) (tetraplatin), a new platinum analogue. PubMed, 48, 1745–1752.

Rose, W.C., Schurig, J.E., Huftalen, J.B., Bradner, W.T., 1982. Antitumor activity and toxicity of cisplatin analogs. PubMed, 66, 135–146.

Rosenberg, B., Vancamp, L., Trosko, J.E., Mansour, V.H., 1969. Platinum compounds: a new class of potent antitumour agents. Nature 222, 385–386.

Salvesen, G.S., 2010. Caspases. Elsevier eBooks, pp. 1297–1302.

Schilder, R.J., LaCreta, F., Perez, R.P., Johnson, S.W., Brennan, J.M., Rogatko, A., et al., 1994. Phase I and pharmacokinetic study of ormaplatin (tetraplatin, NSC 363812) administered on a day 1 and day 8 schedule. PubMed 54, 709–717.

Shalini, S., Dorstyn, L., Dawar, S., Kumar, S., 2014. Old, new and emerging functions of caspases. Cell Death Differ. 22, 526–539.
Shamas-Din, A., Kale, J., Leber, B., Andrews, D.W., 2013. Mechanisms of action of BCL-2 family proteins. Cold Spring Harbor Perspect. Biol. 5, a008714.
Shebaby, W., Elias, A., Mroueh, M., Nehme, B., Jalbout, N.D.E., Iskandar, R., et al., 2020. Himachalol induces apoptosis in B16-F10 murine melanoma cells and protects against skin carcinogenesis. J. Ethnopharmacol. 253, 112545.
Smajilagić, A., Aljičević, M., Redžić, A., Filipović, S., Lagumdžija, A.C., 2013. Rat bone marrow stem cells isolation and culture as a bone formative experimental system. Bosn. J. Basic Med. Sci. 13, 27.
Stătescu, L., Trandafir, L.M., Țarcă, E., Moscalu, M., Constantin, M.M.L., Butnariu, L.I., et al., 2023. Advancing cancer research: current knowledge on cutaneous neoplasia. Int. J. Mol. Sci. 24, 11176.
Trachootham, D., Alexandre, J., Huang, P., 2009. Targeting cancer cells by ROS-mediated mechanisms: a radical therapeutic approach? Nature Reviews. Drug Discover/Nature Reviews. Drug Discovery 8, 579–591.
Wang, D., Lippard, S.J., 2005. Cellular processing of platinum anticancer drugs. Nat. Rev. Drug Discov. 4, 307–320.
Wang, X., 2001. The expanding role of mitochondria in apoptosis. Genes Develop. 15, 2922–2933.
Wang, X., Guo, Z., 2013a. Targeting and delivery of platinum-based anticancer drugs. Chem. Soc. Rev. 42, 202–224.
Wang, X., Guo, Z., 2013b. Targeting and delivery of platinum-based anticancer drugs. Chem. Soc. Rev. 42, 202–224.
Wilkins, H.M., Marquardt, K., Lash, L.H., Linseman, D.A., 2012. Bcl-2 is a novel interacting partner for the 2-oxoglutarate carrier and a key regulator of mitochondrial glutathione. Free Radical Biol. Med. 52, 410–419.
Wilson, J.J., Lippard, S.J., 2013. Synthetic methods for the preparation of platinum anticancer complexes. Retrieved from. http://dspace.mit.edu/handle/1721.1/96862.
Wiśniewski, J.R., Zougman, A., Nagaraj, N., Mann, M., 2009. Universal sample preparation method for proteome analysis. Nat. Methods 6, 359–362.